Empirical Application of Polarimetric Synthetic Aperture Radar for Rice Phenology Monitoring in Irrigated and Favorable Rainfed Ecosystems

Jean Rochielle F. Mirandilla[1 3*], Megumi Yamashita[1], Mitsunori Yoshimura[2]

[1]Graduate School of Agriculture, Tokyo University of Agriculture and Technology, Fuchu, Tokyo 183-8509, Japan; s235342z@st.go.tuat.ac.jp (J.R.F.M); meguyama@cc.tuat.ac.jp (M.Y.)

[2]College of Bioresource Sciences, Nihon University; yoshimura.mitsunori@nihon-u.ac.jp

[3]Philippine Rice Research Institute; jrfmirandilla@exchange.philrice.gov.ph (J.R.F.M)

*s235342z@st.go.tuat.ac.jp

Abstract: *Rice in the Philippines is cultivated under two primary ecosystems: irrigated and rainfed. Rainfed areas can be further categorized as favorable or unfavorable based on rainfall distribution. Management and challenges in production in these ecosystems are observed to be different. This study focused on monitoring rice phenology in irrigated and favorable rainfed ecosystems in Iloilo Province, Philippines, using multi-temporal polarimetric Synthetic Aperture Radar (SAR) data. Multi-temporal SAR datasets were used to capture the temporal dynamics of rice growth across two cropping seasons, 2019 semester 2 and 2020 semester 1. A total of 28 dual polarization SAR images were acquired from Sentinel-1B (C-band, VV and VH polarizations). All images underwent pre-processing, followed by the generation of 2 × 2 covariance matrices, which were analyzed using H/A/alpha decomposition and model-based dual pol decomposition to extract polarimetric parameters. Six key rice growth stages were identified and used to compare the polarimetric bands such entropy, alpha and anisotropy: land preparation, seedling, tillering, reproductive, ripening, and harvested. Statistical analysis such as segmented regression were performed to identify growth-stage-specific changes. The approach enabled the characterization of key phenological stages and the comparison of crop development patterns across the two rice ecosystems. Moreover, notable differences were observed between the backscatter and polarimetric parameters, particularly in relation to water presence in rice paddies. This study demonstrates the potential of dual-polarization SAR for operational rice monitoring and for distinguishing phenological behavior under different water management regimes in rice ecosystems.*

Keywords: Irrigated Rice Ecosystem, Favorable Rainfed Rice Ecosystems, Polarimetric SAR, Sentinel-1B

Introduction

Rice is grown in various ecosystems—irrigated, rainfed, and upland—classified according to terrain and water accessibility in the rice fields (IRRI, 1993). These different ecosystems influence rice productivity and even climate change agriculture interface. Irrigated rice has a higher yield level than the other rice ecosystems due to the consistent water availability in rice growing season. Moreover, irrigated rice fields with continuously flooded are documented to be major contributors of methane emission due to sustained anaerobic soil conditions, while rainfed rice with alternate wetting and drying has a lower level of methane gas production (Cowan et.al., 2021). With these differences, monitoring rice fields according to their ecosystems will help to increase production and properly manage the

cause-and-effect of climate change. Delineation of these rice ecosystems can give rice stakeholders to properly address the yield gaps and mitigation strategies to minimize the effect of climate change.

Synthetic Aperture Radar (SAR) has advantage in agricultural monitoring due to its ability to penetrate clouds during growing season. Sentinel-1, a C-band SAR system operated by European Space Agency (ESA) is operating in dual polarization that provides data for rice monitoring in the Philippines. In an instance, Philippine Rice Information System, a rice monitoring system under the Philippine rice Research Institute, uses Sentinel-1 for rice detection, area and yield estimation. It uses ruled-based rice detection using the multi-temporal backscatter and its relationship to rice stages (Nelson, et al., 2014, Mabalay, et al., 2022).

In recent years, polarimetric decomposition techniques can enhance SAR data interpretation through separation of scattering mechanisms for instance surface scattering, double-bounce and volume scattering (Cloude & Pottier, 1996). This is significant for different rice ecosystems, the growth and water availability strongly influence the scattering signatures. Irrigated rice fields are flooded and often have dense canopies frequently show strong double-bounce and volume scattering, while rainfed fields with unstable water availability and less dense vegetation can exhibit different scattering responses (Nelson et al., 2014; Nguyen et al., 2020). It is possible to capture these scattering differences by performing polarimetric decomposition techniques such as Free-man-Durden and Cloude-Pottier.

This study, therefore, focuses on the use of polarimetric decomposition to monitor irrigated and favorable rainfed rice ecosystems, highlighting their differences to support both productivity enhancement and climate change mitigation strategies.

Literature Review

Synthetic Aperture Radar (SAR) is an active remote sensing technology that uses microwave signals to capture detailed images of Earth's surface. In contrast to optical sensors, it has the capacity to capture data regardless of weather conditions such as cloud cover. SAR systems transmit their own radar pulses and record the backscattered signals to return to the sensor (Richards, 2009). Generally, the backscatter intensity is used for vegetation monitoring, especially in rice, as it has a unique backscatter trend (Nelson et al., 2014, Mabalay et al., 2022). Recently, Polarimetric Synthetic Aperture Radar (PolSAR) has been studied to be used as a tool in agricultural monitoring. PolSAR refers to the measurement and analysis of

the polarization state of signals, which offers valuable insights into surface structure, geometry, and material properties. As radar waves interact with different ground targets, their polarization state may change, thereby providing additional information about the Earth's surface (eoPortal, 2025).

The application of polarimetric decomposition techniques, such as H-A-α (Cloude-Pottier decomposition) and model-based methods, allows for the extraction of scattering parameters that are sensitive to crop structure and growth stages. These parameters, including entropy, anisotropy, and alpha angle, offer insights into the dominant scattering mechanisms within rice fields (Ji & Wu, 2015, Harfenmeister et al., 2020, Mascolo et al., 2020, Wang et al., 2023, Dave et al., 2023). Studies showed that the polarimetric parameters of the temporal profiles are sensitive to the changes in plant appearance and biophysical parameters with the phenological development of crops such as wheat and barley (Harfenmeister et al., 2020, Wang et al., 2023), rice (Dave et al., 2023), and forest (Sugimoto et al., 2023). For example, low entropy and alpha angle values are observed during early growth stages, which indicated the dominant surface scattering mechanism, while higher values during later stages suggested increased volume scattering due to canopy development (Ji & Wu, 2015, Harfenmeister et al., 2020).

In addition, estimation of the vegetation biomass (Jesus et al., 2022), classification of different vegetation (Shao et al., 2012, Haldar et al., 2018) and soil moisture retrieval (Merzouki et al., 2018) were tested using the polarimetric decomposition. For example, Haldar et al. (2018) showed that using single date full polarimetric SAR data with different decomposition techniques can improve the discrimination of heterogenous agricultural.

In general, polarimetric decomposition methods offer useful data for monitoring crop growth and differentiating among different crops. The potential of PolSAR in precision agriculture was shown from its capabilities to detect the crop stages and scattering parameters' sensitivity to crop biophysical characteristics. Improvement of decomposition techniques and machine learning algorithm integration may increase the use of PolSAR in various agricultural contexts and the classification accuracy.

Methodology

I. Study Site and Data

A total of forty (40) monitoring fields were selected in the province of Iloilo, Philippines, 20 rice fields each in irrigated and favorable rainfed rice fields (Table 1). The selection of monitoring fields was based on the monitoring sites from Philippine Rice Information

System Project. These fields were continuously monitored since 2016. The province of Iloilo (Figure 1) is located in the center of the Philippine archipelago (10.69694º N, 122.56444º E). It is considered as the rice granary of the region as rice is the major crop in the province (Province of Iloilo). It has a type of Type 3 climate which is defined as seasons are not very pronounced, relatively dry from November to April, and wet during the rest of the year.

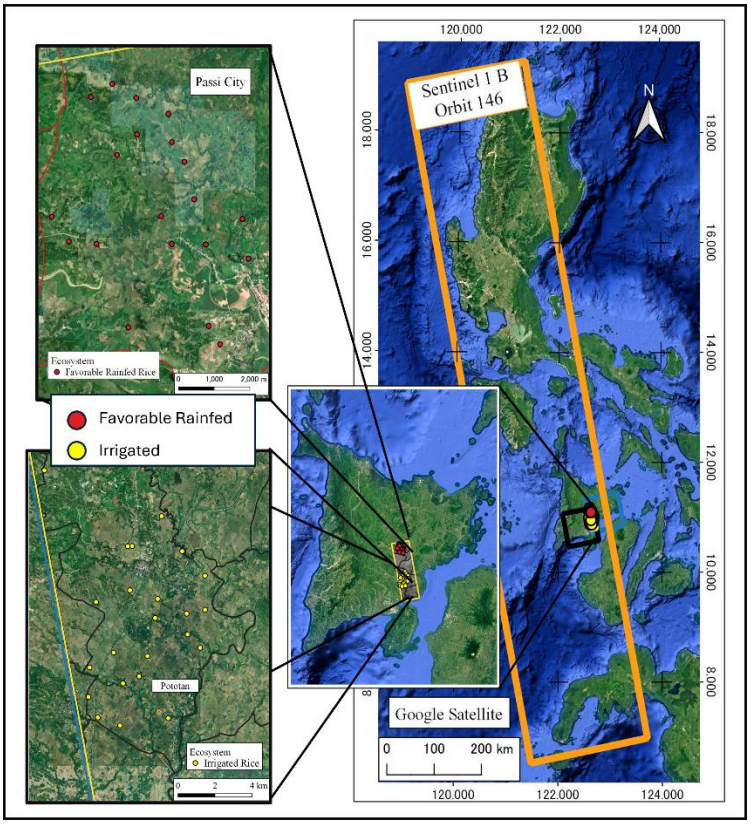

Figure 1. The study rice monitoring fields, Sentinel-1B orbit frames in the province of Iloilo, Philippines

Table 1. Number of monitoring fields used from 2019 Semester 2 to 2020 Semester 1

Municipalities in	Monitoring Field (MF)	
Iloilo, Philippines	Number of fields	Ecosystem
Passi City	20	Favorable Rainfed
Pototan	20	Irrigated
Total	40	

The daily weather data such as precipitation (mm/day) of the province was down-loaded from the National Aeronautics and Space Administration (NASA) Langley Re-search Center (LaRC) Prediction of Worldwide Energy Resource (POWER) Project funded through the NASA Earth Science/Applied Science Program. Precipitation data was used in monitoring especially in rainfed rice ecosystems that depend on it for source of irrigation.

II. Synthetic Aperture Radar

There are two planting semesters in the Philippines based on the planting schedule, Semester 1 covers planting dates from September 16 to March 15, while Semester 2 spans from March 16 to September 15 (Gutierrez et al., 2019). The study used 28 images of Sentinel-1B, a C-band SAR developed by European Space Agency (ESA) sensor with 5.6 cm wavelength and 12 days revisit period. These images were downloaded from Copernicus Sentinel Open Access Hub. It runs dual polarization across the area of interest in Iloilo, Philippines, VH and VV polarization. The monitoring fields and satellite frames/orbits are shown in Figure 1, and the satellite properties are summarized in Table 2.

Table 2. Satellite used in the study and its properties.

SAR imagery	Number of images used	Orbit/Frame	Flight Direction	Midswath incidence/Off-Nadir Angle	Resolution	Product Level	Polarization
Sentinel-1B	28	146	Ascending	39.0	10 m	SLC IW Level 1	VH, VV

Sentinel-1B was pre-processed in the ESA Sentinel Application Platform (SNAP 11.0) software as shown in Figure 2. Polarimetric decomposition was originally developed for full polarization data, however with the limited source of these data several methods were developed to extract them in dual polarization SAR (Ji, K., & Wu, Y., 2015). In this study, two dual polarization (dual pol) polarimetric decomposition were used, H-A-Alpha decomposition and model-based dual pol decomposition. H-A-Alpha decomposition is a modified form of the Cloude–Pottier method adapted for dual-polarization SAR. It derives three parameters, entropy, anisotropy and alpha, through the eigenvalue-eigenvector analysis of the coherency matrix. These parameters qualitatively characterize the scattering mechanisms: entropy (H) quantifies the randomness of scattering, anisotropy (A) indicates the relative contribution of secondary scattering mechanisms, and alpha angle (α) identifies the dominant scattering type (Ji & Wu, 2015, Harfenmeister et al., 2020, Wang et al., 2023). In contrast, model-based dual-pol decomposition, based on the Stokes vector formalism, separates dual-polarization data into distinct scattering mechanisms, providing quantitative estimates of scattering powers and related polarimetric parameters (Ji & Wu, 2015, Mascolo

et al., 2022). In SNAP, this method generates seven parameters: alpha (α), delta (δ), ratio, rho (ρ), span, surface scattering, and volume scattering.

The preprocessing chain used for Sentinel-1B (S1B) included importing of the SAR images to SNAP, orbit file application, TOPSAR split, calibration, TOPSAR deburst, polarimetric speckle filter application, polarimetric decomposition, multi-look, terrain correction and extraction of different polarimetric parameters. To provide the actual satellite positioning, orbit file was applied to the Sentinel-1 Single Look Complex (SLC) Level 1 product. With the three sub-swaths (IW1, IW2, IW3), the area of interest was selected using the TOPSAR split function, then the images were calibrated. TOPSAR deburst was needed to merge all bursts into seamless images. Polarimetric speckle filter, refined lee filter with 5x5 window size, and multi-look (azimuth looks: 1 and range looks: 4) was performed after performing polarimetric decomposition to acquire better SAR quality and make the pixel square. Lastly, to convert the image into UTM Zone 51N map coordinate system, terrain correction was applied. All preprocessed images were stacked using co-register tool to perform further analysis. Polarimetric values were extracted from the 40 monitoring fields for phenology trends and statistical analysis.

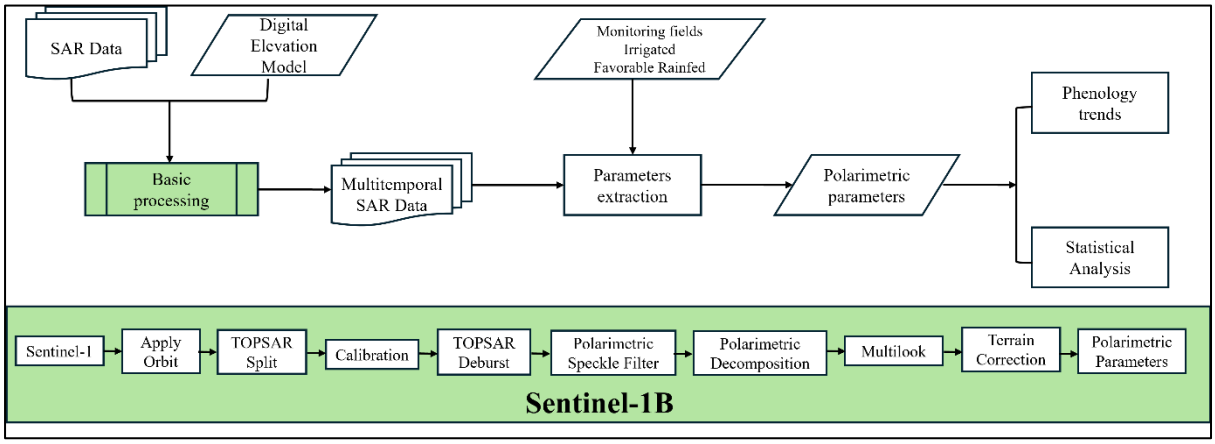

Figure 2. Workflow of the study

Segmented regression, piecewise linear regression, models the data using multiple linear segments instead of a single line by identifying breakpoints where the relationship between variables shifts (Darabi, 2024). This approach is useful for detecting breakpoints that correspond to changes in rice phenology within each ecosystem. It also enables the examination of linear trends and phenology-specific dynamics in SAR signals.

RGB composite images were generated from model-based dual pol decomposition using the key parameters; surface scattering as red (R) band, volume scattering as green (G) band,

and span as blue (B) band. These images were to illustrate the field conditions in the area of interest in the province of Iloilo, Philippines.

Results and Discussion

I. Ground data from monitoring rice fields

A total of 40 monitoring fields from the Philippine Rice Information System (PRiSM) project were used as the ground validation points. These are from the favorable rainfed rice ecosystem of Passi City and irrigated rice ecosystem in Pototan, both are municipalities within the province of Iloilo, Philippines (Table 3). Mostly farmers established inbred varieties with early maturity days (93 – 104 days) using direct-seeded method. The municipalities had different peak of establishment and harvesting months, however in each municipality the farmers planted within the month.

Table 3. Summary of monitoring ground data from 2019 Semester 2 (S2) to 2020 Semester 1 (S1).

Details	Favorable Rainfed Rice		Irrigated Rice	
	2019Sem2	2020Sem1	2019Sem2	2020Sem1
Municipality	Passi City		Pototan	
Number of monitoring fields	20		20	
Variety	Inbred		Inbred/Hybrid	
Rice variety maturity days (Average)	93	90	104	99
Majority of establishment method	Direct seeded		Direct seeded	
Peak of establishment month (SoS[1] month)	June	October	July	November
Peak of harvesting month (EoS[2] month)	September	January	October	March

[1] SoS – Start of Semester, [2] EoS – End of Semester

II. Polarimetric parameters phenological trends

The key parameters from the two polarimetric decomposition methods used in the study were extracted from the monitoring fields in irrigated and favorable rainfed rice ecosystem. As shown in Figure 3, the different key parameters were presented against the days of year to show the phenological trend for 2 planting semesters. The different colored lines represent each monitoring field in each rice ecosystem while black line represents the average values. The blue bar represents the precipitation (mm/day) downloaded from NASA POWER.

All three key parameters (entropy, anisotropy, alpha angle) obtained from the H-A-Alpha decomposition were presented while only selected three key parameters from model-based dual pol decomposition (ratio, surface scattering, volume scattering) presented in this paper. These were selected based on the results of the segmented regression.

Two distinct peaks and dips can be seen in the temporal trend of entropy, anisotropy, alpha angle and ratio which indicated that there were two planting semesters in the irrigated and favorable rainfed rice ecosystems. Based on the ground data, entropy and alpha angle had the same trend, low values in after the establishment period and high values in ripening or harvesting period. In contrast to anisotropy and ratio parameters with increasing values from establishment to seedling and decreasing values from ripening to harvesting period. Surface scattering and volume scattering trends were quite variable in each rice stage in both irrigated rice and favorable rainfed rice ecosystems.

Entropy is the measurement of randomness in the scattering which ranges from 0 to 1, 1 means it is more complex scattering (Ji & Wu, 2015, Harfenmeister, et al., 2020). The entropy's values in irrigated ranged from 0.3 to 0.9 while favorable rainfed rice ranged from 0.4 to 0.9. Following crop establishment, low entropy values indicate that scattering was dominated by a single mechanism, either surface or double-bounce. By contrast, during the harvesting period, entropy reached moderate to high levels, reflecting greater randomness and contributions from multiple scattering mechanisms.

Anisotropy had contradicting trend with entropy, with values ranged from 0.3 to 0.9 and 0.4 to 0.8, in irrigated rice and favorable rainfed rice, respectively. After the establishment period the anisotropy in both irrigated and favorable rainfed rice had high values while in harvesting period it had low values. Interpretation of anisotropy is often interpreted and analyzed alongside with entropy (Ji & Wu, 2015).

Similar from entropy, alpha followed the temporal trend in both irrigated and favorable rainfed rice observed with low values after the establishment period and higher in harvesting period. The alpha angle (°) represents the average scattering mechanism of the target and is used to classify the dominant scattering type, such as surface, volume, or double-bounce scattering. Lower values (close to 0°) reflect that the dominant mechanism is surface scattering, values near 45° indicate volume scattering, and those approaching 90° reflect double-bounce scattering (Ji & Wu, 2015, Harfenmeister, et al., 2020). In both irrigated and favorable rainfed ecosystems, alpha values ranged from 5° to 38°. The results suggest that predominant scattering mechanisms were surface and volume scattering. Surface scattering

was more evident after crop establishment (low values), whereas volume scattering was dominant during the harvesting period (higher values).

H-A-Alpha decomposition parameters qualitatively characterize the scattering mechanisms so they can be interpreted together. Low entropy and low alpha angle mean that the area is dominated by surface scattering such as bare ground and calm water while low entropy and high alpha angle mean it was dominated by double-bounced scattering. High entropy with intermediate alpha represents that volume scattering is dominant (e.g. forest, crops) (Koppe et. Al., 2013, Ji & Wu, 2015, Harfenmeister, et al., 2020, Mascolo et al., 2022, Wang et al., 2023). Based on the results, after the establishment the entropy and alpha angle had low values, which means the dominant scattering mechanism is surface scattering. This is due to the farmers' management during these stages, the farmers kept the rice field saturated during the establishment (direct-seeded) then flooded the rice field after the seeds sprouted to prevent weeds from growing. The seedlings were thin and the signal couldn't be attenuated by them. In contrast, in harvesting period had high entropy and moderate alpha angle, which can indicate that volume scattering was the dominant scattering mechanism. This can be because of the rice stubbles present in the rice field after the harvest. The farmers in the area still practice manual harvesting which make a taller rice stubbles remaining in the rice field.

This study also used model-based dual pol decomposition to extract parameters providing quantitative estimates of scattering powers. Figure 3 showed the three selected key parameters from this method, ratio, surface scattering and volume scattering. Ratio followed the same temporal trend with anisotropy, high values after the establishment and low values in the harvesting period. On the other hand, surface scattering and volume scattering had a variable trend in irrigated rice and favorable rainfed rice ecosystems.

Based on the results, surface scattering is ranged from -8 to -21 and -9 to -23 from the establishment to harvesting period, irrigated rice and favorable rainfed rice, respectively. It showed that surface values in the individual favorable rainfed rice field exhibited more variability than the irrigated rice. In addition, the surface scattering values generally increased in accordance with rainfall events. This is due to the fact that rainfall events influenced the irrigation water in the rice fields, especially in the favorable rainfed rice which is dependent on rainfall for irrigation. Same as surface scattering, the volume scattering in both irrigated and favorable rainfed rice ecosystems show peaks following rainfall events, especially in favorable rainfed rice. Furthermore, volume scattering was more variable in the favorable rainfed rice than in irrigated rice ecosystem. This really

showed that presence of irrigation water can affect the scattering mechanisms in the rice fields.

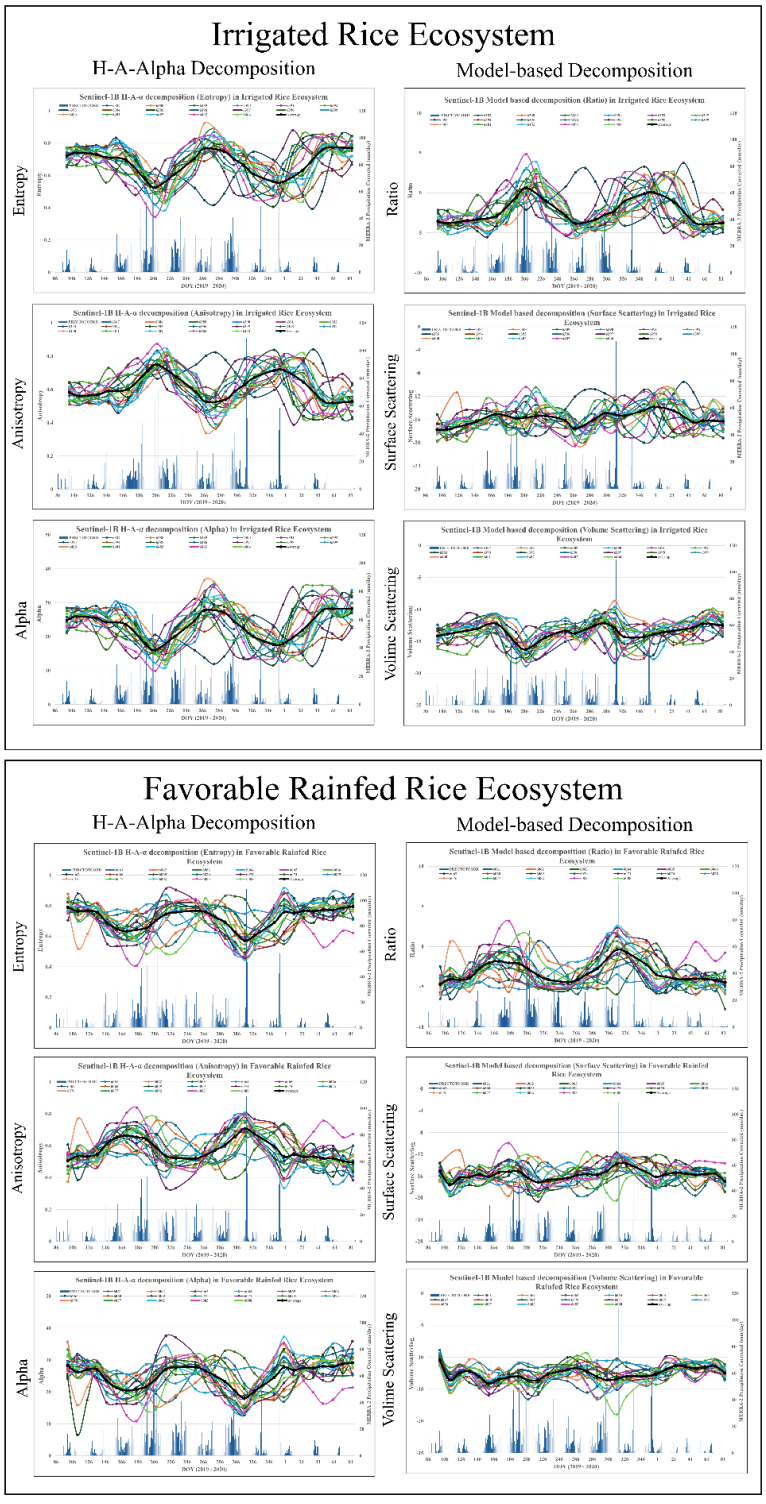

Figure 3. Polarimetric parameters trends generated from H-A-Alpha decomposition (entropy, anisotropy and alpha angle) and model-based dual pol decomposition (ratio, surface scattering and volume scattering) in the irrigated rice and favorable rainfed rice ecosystems.

III. Polarimetric parameters and Rice stages

Polarimetric values were extracted from the monitoring rice fields in specific rice stages/phases. Rice stages/phases images were identified for each monitoring field based on the known establishment and harvesting dates. As shown in Figure 4, the statistical data from each rice ecosystem and selected polarimetric parameters. Segmented regression was performed to the polarimetric parameters from Sentinel-1B to check the relationship between the polarimetric parameters and rice stages/phases. The results showed that there are one to two breakpoints in polarimetric parameters in irrigated rice and favorable rainfed rice ecosystems. Breakpoints (ψ) are shown in the broken lines inside the graph with the number representing rice stages/phases, 1 – land preparation, 2 – seedling, 3 – vegetative, 4 – flowering, 5 – ripening, and 6 – harvested.

The box-and-whisker plots provided the summary of the distribution of polarimetric parameters across irrigated and favorable rainfed rice ecosystems (Figure 4). The mean line showed the phenology trend while the box (interquartile ranges) showed the variability in the parameters in different rice stages/phases. Generally, irrigated rice exhibited narrower box than favorable rainfed rice which can indicate stable scattering dynamics under controlled irrigation. In contrast, favorable rainfed rice showed wider variability and more dispersed outliers, which may indicate the influence of irregular variability due to rainfall availability. These distinctions were evident in entropy, anisotropy, alpha at ratio, irrigated rice showed more predictable temporal patterns, whereas favorable rainfed rice has flatter trend and higher variability. As discussed in earlier section, entropy and alpha angle exhibited similar the same phenology trend, low values after the establishment, increased from tillering to flowering and slightly decreased in harvested stage. In contrast, the temporal trends of anisotropy and ratio displayed opposite patterns to those of entropy.

The summary of the breakpoints and model resulted from the segmented regression analysis is shown in Table 4. The breakpoints were generally exhibited in the seedling to tillering and flowering to ripening stages. This is probably due to the physical change in these stages, such as increasing tillers (stems) and leaves and immerging of panicles in the flowering to ripening stages. Based on the results, the RMSE of the polarimetric parameters across the rice growth stages/phases were low to moderate model fit. Among the parameters, anisotropy in irrigated rice achieved the best fit, with an R^2 of 0.59 and an RMSE of 0.07, whereas surface scattering in irrigated rice showed the weakest fit, with an R^2 of 0.03 and an RMSE of 2.02. Generally, in Sentinel-1B polarimetric parameters,

favorable rainfed rice ecosystem got a better fit model with the rice growth stages compared to the irrigated rice ecosystems. This can be due to more complicated phenology trend in irrigated rice compared to the flatter trend of polarimetric parameters in favorable rainfed rice.

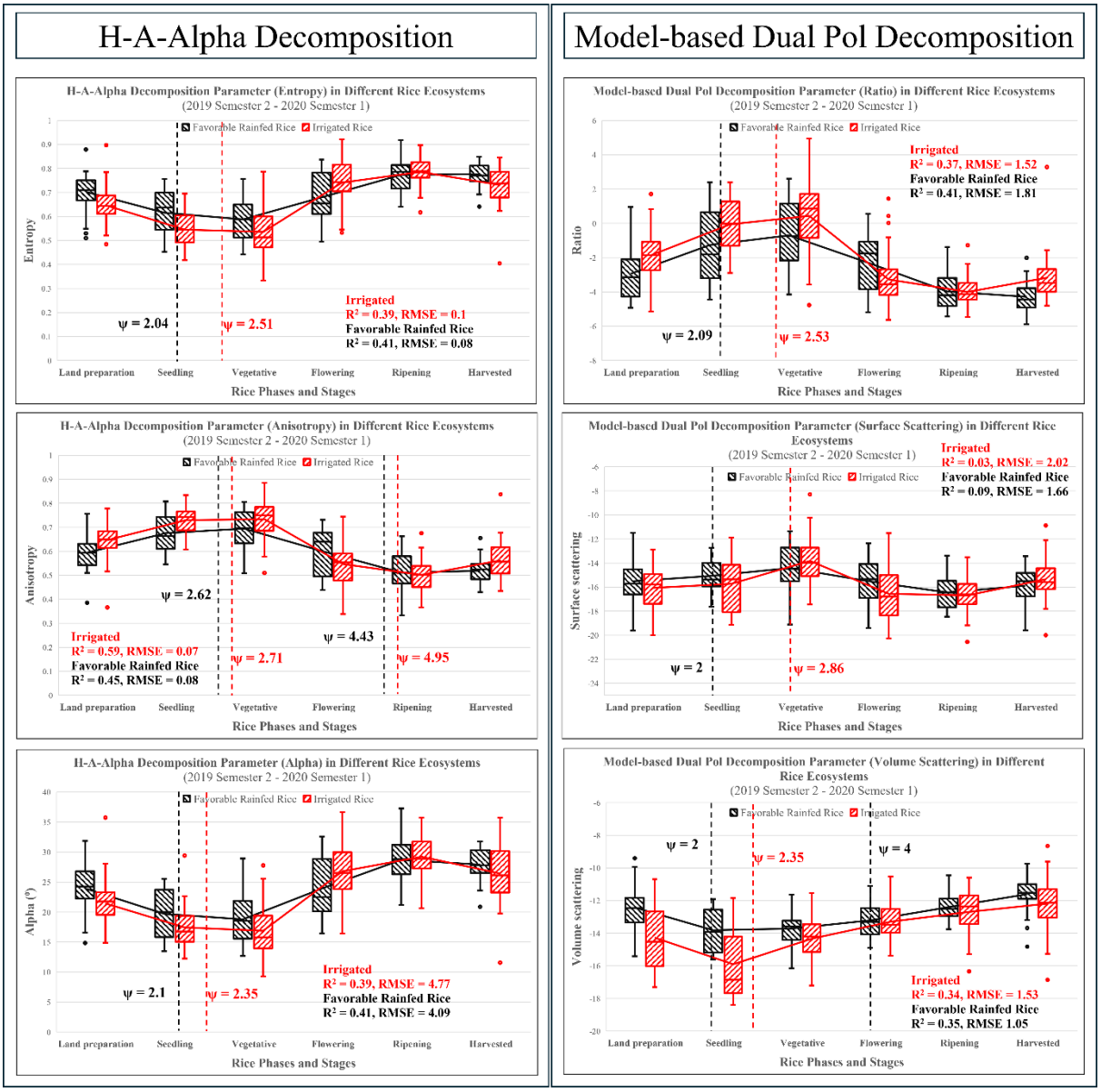

Figure 4. Box-and-whisker plots of selected polarimetric parameters across irrigated and favorable rainfed rice ecosystems with the breakpoints identified through segmented regression analysis.

IV. RGB composite monitoring

RGB composite images derived from Sentinel-1B model-based dual pol decomposition were generated to illustrate field conditions at the time of each satellite acquisition. The composites were constructed using surface scattering in the red band, volume scattering in

the green band, and the ratio in the blue band. Eight acquisition dates were selected and presented in Figure 5, (a) June 21, 2019, (b) July 15, 2019, (c) August 20, 2019, (d) September 25, 2019, (e) October 15, 2019, (f) November 24, 2019, (g) December, 18, 2019, and (h) February 16, 2020. Images were zoomed to highlight the different rice ecosystems in the area of interest, the irrigated rice in Pototan, and the favorable rainfed rice in Passi City.

The RGB composite images effectively showed the differences in the rice growth stages within the rice ecosystems. The images reflected the distinct color variations resulting from differences in scattering mechanisms in the rice fields in the different rice growth stages/phases. As shown in Figure 5, the composites displayed a pink color during the land preparation to establishment and early tillering stages. For example, on June 21, 2019 (Figure 5a), most favorable rainfed rice fields appeared pink, while on July 15, 2019 (Figure 5.b) and November 24, 2019 (Figure 5f), the majority of irrigated fields exhibited the same color pattern, reflecting their land preparation stage to establishment period. The pink coloration resulted from strong surface scattering (red band) combined with moderate contributions from volume scattering (green band), which dominated during these early growth phases. This was same results as mentioned in the earlier section; establishment period has higher surface scattering values.

Green color appeared in the RGB composite images during the tillering to ripening stages in the rice fields as observed in Figure 5.c (August 20, 2019) and November 24, 2019 (Figure 5.f) in the favorable rainfed rice. This green tone reflects the dominance of volume scattering, which is strongly influenced by the increasing biomass and canopy density during the vegetative phase (Ji & Wu, 2015).

In contrast, cyan-blue can be seen in the ripening stages in the irrigated rice on February 16, 2020 (Figure 5.h). In these fields indicated mixture of volume and surface scattering and high ratio values, which can correspond to the drying of panicles and reduced vegetation water content toward maturity. The RGB composite images captured the phenological transition from active vegetative growth to the final grain-filling and ripening stages. Effectively highlighting the sensitivity of dual-pol decomposition to rice growth dynamics.

Figure 5. RGB composite of Sentinel-1B showing the monitoring fields in favorable rainfed rice and irrigated rice ecosystems (R: Surface scattering, G:Volume scattering, B: Ratio)

Conclusion and Recommendation

This study demonstrated the potential of polarimetric SAR decomposition parameters from Sentinel-1B for monitoring irrigated and favorable rainfed rice ecosystems in selected municipalities in Iloilo, Philippines. Two decomposition methods for dual polarization were used, H-A-Alpha decomposition (entropy, anisotropy, alpha angle) and model-based dual pol decomposition (ratio, surface scattering, and volume scattering). The different polarimetric parameters captured distinct phenological trends across two planting seasons. Results showed that entropy and alpha angle consistently increased from crop establishment to harvesting with lower values after the establishment period and peaked during the flowering stage. In contrast, anisotropy and ratio displayed opposite temporal trend, high values during establishment and seedling stages decreased during the ripening and harvested period.

The combination of polarimetric SAR decomposition parameters can effectively monitor the phenological stages in irrigated and favorable rainfed rice ecosystems. In instance, in a high entropy value in combination with low alpha angle showed that the rice fields were in the establishment to early tillering stages. This is due to the dominant surface scattering mechanism in the rice fields. Meanwhile, in low entropy and moderate alpha angle can indicate that the rice fields are in maximum tillering to ripening stages.

Furthermore, RGB composites (R: surface scattering, G: volume scattering, B: ratio) of dual-pol decomposition further highlighted these stage-specific scattering mechanisms, enabling clear visualization of phenological transitions. Irrigated rice tends to exhibit more stable transitions from red, green to blue, while favorable rainfed rice shows patchier or less intense color shifts, reflecting variability in water availability and crop development. Pink color in the field can indicate that the rice fields are in establishment to early tillering stages, which the rice fields are flooded with small rice plants. Surface scattering is dominant mechanism as irrigation water and seedlings have less signal interaction. Cyan - blue colors can be seen during the peak of planting or during the flowering to ripening stages, which can indicate high ratio values and dense canopy.

Moreover, comparisons between ecosystems showed that irrigated rice exhibited relatively stable scattering signatures, while favorable rainfed rice displayed greater variability, particularly in surface and volume scattering, due to its dependence on rainfall events. These findings underscore the sensitivity of polarimetric parameters to both phenological stages and water availability, highlighting their effectiveness for rice ecosystem

discrimination.

Recommendations: To improve the different ecosystems discrimination, future research can integrate polarimetric SAR parameters with other optical indices and crop growth models. Integrating more sensors such as L-band SAR and full polarization SAR may improve rice stage detection and rice ecosystems characterization. These parameters can help properly in discrimination irrigated from rainfed rice. Machine learning approaches such as Random Forest or deep learning should be employed to operationalize ecosystem classification and extend monitoring to larger scales. These advancements will enhance the application of SAR in supporting rice productivity assessment, climate adaptation, and food security planning.

References

Reference to an article in online journals or online first [DOI]:

Darabi, H., Haghighi, A. T., Klöve, B., & Luoto, M. (2024). Remote sensing of vegetation trends: A review of methodological choices and sources of uncertainty. Remote Sensing Applications: Society and Environment, 37, 101500. https://doi.org/10.1016/j.rsase.2025.101500

Dave, Rucha & Saha, Koushik & Kushwaha, Amit & Vithalpura, Manisha & Parath, Nidhin & Murugesan, Abishek. (2023). Analysing the potential of polarimetric decomposition parameters of Sentinel–1 dual-pol SAR data for estimation of rice crop biophysical parameters. Journal of Agrometeorology. 25. 10.54386/jam.v25i1.2039. 29

Gutierrez, M. A., Paguirigan, N. M., Raviz, J., Mabalay, M. R., Alosnos, E., Villano, L., ... & Laborte, A. (2019). The rice planting window in the Philippines: an analysis using multi-temporal SAR imagery. The International Archives of the Photogrammetry, Remote Sensing and Spatial Information Sciences, 42, 241-248.

Haldar, D., Dave, R., & Dave, V. A. (2018). Evaluation of full-polarimetric parameters for vegetation monitoring in rabi (winter) season. The Egyptian Journal of Remote Sensing and Space Science, 21, S67-S73. https://doi.org/10.1016/j.ejrs.2018.05.002

Harfenmeister, K., Itzerott, S., Weltzien, C., & Spengler, D. (2020). Agricultural Monitoring Using Polarimetric Decomposition Parameters of Sentinel-1 Data. Remote Sensing, 13(4), 575. https://doi.org/10.3390/rs13040575

Jesus, J. B. D., Kuplich, T. M., Barreto, Í. D. D. C., & Gama, D. C. (2022). Dual polarimetric decomposition in Sentinel-1 images to estimate aboveground biomass of arboreal caatinga. Remote Sensing Applications: Society and Environment, 29, 100897. https://doi.org/10.1016/j.rsase.2022.100897

Ji, K., & Wu, Y. (2015). Scattering Mechanism Extraction by a Modified Cloude-Pottier Decomposition for Dual Polarization SAR. Remote Sensing, 7(6), 7447-7470. https://doi.org/10.3390/rs70607447

Koppe, W., Gnyp, M. L., Hütt, C., Yao, Y., Miao, Y., Chen, X., & Bareth, G. (2013). Rice monitoring with multi-temporal and dual-polarimetric TerraSAR-X data. International

Journal of Applied Earth Observation and Geoinformation, 21, 568-576. https://doi.org/10.1016/j.jag.2012.07.016

Mascolo L., S. R. Cloude and J. M. Lopez-Sanchez, (2022) "Model-Based Decomposition of Dual-Pol SAR Data: Application to Sen-tinel-1," in IEEE Transactions on Geoscience and Remote Sensing, vol. 60, pp. 1-19, 2022, Art no. 5220119, doi: 10.1109/TGRS.2021.3137588.

Merzouki, A., McNairn, H., Powers, J., & Friesen, M. (2018). Synthetic Aperture Radar (SAR) Compact Polarimetry for Soil Moisture Retrieval. Remote Sensing, 11(19), 2227. https://doi.org/10.3390/rs11192227

Nelson, A., Setiyono, T., Rala, A. B., Quicho, E. D., Raviz, J. V., Abonete, P. J., Maunahan, A. A., Garcia, C. A., Bhatti, H. Z., Villano, L. S., Thongbai, P., Holecz, F., Barbieri, M., Collivignarelli, F., Gatti, L., Quilang, E. J., Mabalay, M. R., Mabalot, P. E., Barroga, M. I., . . . Ninh, N. H. (2014). Towards an Operational SAR-Based Rice Monitoring System in Asia: Examples from 13 Demonstration Sites across Asia in the RIICE Project. Remote Sensing, 6(11), 10773-10812. https://doi.org/10.3390/rs61110773

Y. Shao, K. Li, R. Touzi, B. Brisco and F. Zhang, "Rice scattering mechanism analysis and classification using polarimetric RADARSAT-2," 2012 IEEE International Geoscience and Remote Sensing Symposium, Munich, Germany, 2012, pp. 1445-1448, doi: 10.1109/IGARSS.2012.6351263.

Sugimoto, R., Nakamura, R., Tsutsumi, C., & Yamaguchi, Y. (2022). Extension of Scattering Power Decomposition to Dual-Polarization Data for Tropical Forest Monitoring. Remote Sensing, 15(3), 839. https://doi.org/10.3390/rs15030839

Wang, M., Wang, L., Guo, Y., Cui, Y., Liu, J., Chen, L., Wang, T., & Li, H. (2023). A Comprehensive Evaluation of Dual-Polarimetric Sentinel-1 SAR Data for Monitoring Key Phenological Stages of Winter Wheat. Remote Sensing, 16(10), 1659. https://doi.org/10.3390/rs16101659

Reference to a book (ISBN):

International Rice Research Institute (IRRI). 1993. Rice research in a time of change. IRRI, Los Baños, Laguna, Philippines.

Mabalay, M. R., Raviz, J., Alosnos, E., Barbieri, M., Quicho, E., Bibar, J. E. A., ... & Laborte, A. (2022). The Philippine Rice In-formation System (PRiSM): an operational monitoring and information system on rice. Remote Sensing of Agriculture and Land Cover/Land Use Changes in South and Southeast Asian Countries, 133.

Richards, J.A. (2009) Remote Sensing with Imaging Radar. Signals and Communication Technology. Springer-Verlag, Berlin. http://dx.doi.org/10.1007/978-3-642-02020-9

For Internet resources:

Province of Iloilo (created 11/07/2021) About Iloilo Retrieved September 2, 2025 from https://www.iloilo.gov.ph/en/about-iloilo

eoPortal. (updated May 14, 2025). Other Space Activities. EOPortal. Retrieved September 5, 2025 from https://www.eoportal.org/other-space-activities.